

SOME DESIGNS OF THE GAIA DETECTOR SYSTEM¹

E. Høg

Copenhagen University Observatory
Østervoldgade 3, 1350 Copenhagen K, Denmark
Electronic mail: erik@astro.ku.dk

ABSTRACT

Some new CCD detector systems for the *interferometric* part of GAIA are described as basis for further studies; problems of the proposed CCD design are pointed out. A detector concept was originally described by Lindegren & Perryman (1994) but was of course not yet optimized. The present study shows its potential for further improvements. The new systems are optically simpler, e.g., the suggested plate with 800 millimeter-size field lenses on each of 32 fields in the focal plane are not required in the new detector for an amplitude grid. In case of a phase grid a plate with only 20 cylinder field lenses is sufficient. The efficiency will be near to the theoretical maximum set by the QE of the CCD. An integration time per CCD of for instance one second is possible by the proposed ‘*drift-scan modulation detector*’, compared to 0.2 s for the original system. It appears that that an input catalogue of the expected 50 million program stars is required for the interferometric observations. A data transmission rate to the ground of about 250 kbits/s is indicated, after a certain preprocessing on-board. – An input catalogue of about one million bright stars observed by the detectors in the *incoherent* imaging mode of the outer part of the field would be sufficient for the purpose of real time attitude determination.

Keywords: space astrometry; interferometry; GAIA; detector system.

1. INTRODUCTION

Principles of a detection system for GAIA have been outlined by Lindegren & Perryman (1994), hereafter referred as LP. The authors describe two possible kinds of grids, an amplitude grid and a phase grid, cf. LP-Fig. 6. The phase grid has the higher detection efficiency of the two and it has been assumed in the performance given in LP-Table 3. LP furthermore propose to measure the modulation by a CCD with eight memory pixels to store the eight phases of the light curve during integration over many modulation cycles. This principle was originally

proposed and illustrated by Høg & Lindegren (1993) and it is here adapted to the application with GAIA.

Our Fig. 1b shows the principle of light modulation, derived from LP-Fig. 6, but with the filter and masks added for reasons of clarity.

2. DETECTOR DESIGN #1 – FOR AN AMPLITUDE GRID

A new CCD detector for GAIA is proposed. It is optically simpler than the one proposed by LP-Fig. 6A since no field lenses are required.

The principle of light modulation is shown in Fig. 1. (a) refers to the present proposal and (b) shows for comparison the proposal by LP-Fig. 6. The modulation grid has the same period as the interference fringes in the diffraction image of the star. As the image moves due to satellite rotation the transmitted light is modulated as shown by the lower curve in (a). This light hits a large pixel of a CCD, and sometimes an opaque layer covering a memory pixel, as shown. In order to measure the modulation curve the charge accumulated in the pixel is shifted into a memory pixel after one eighth of a period so that only little smearing of the phase information will take place.

The eight charges, each corresponding to a certain phase of the modulation curve must be stored in eight memory pixels of the CCD. The CCD must also be able to accumulate many integrations at the same phase while the star is passing the detector pixel. Figure 2 shows a CCD with this capability.

Figure 2a shows one of the 32 fields in the focal plane of GAIA, i.e., in the central part destined for interferometric measurement, cf. LP-Fig. 7. A field is divided into 20×40 subfields of size $27'' \times 13.5''$, as in Fig. 2b. A star will cross a subfield in 225 ms with the proposed rotation speed of 120 arcsec/s for the satellite. The field is covered with a modulation grid having a period about 0.003 mm or 54 mas, i.e., 500 slits per subfield. The grid period corresponds to 0.450 ms. The detector and memory pixels corresponding to a subfield are shown enlarged in Fig. 2c, and a small part of this is further enlarged in Fig. 2d.

¹A contribution to *Future Possibilities for Astrometry in Space*, a workshop at RGO, Cambridge, England, 19-21 June 1995

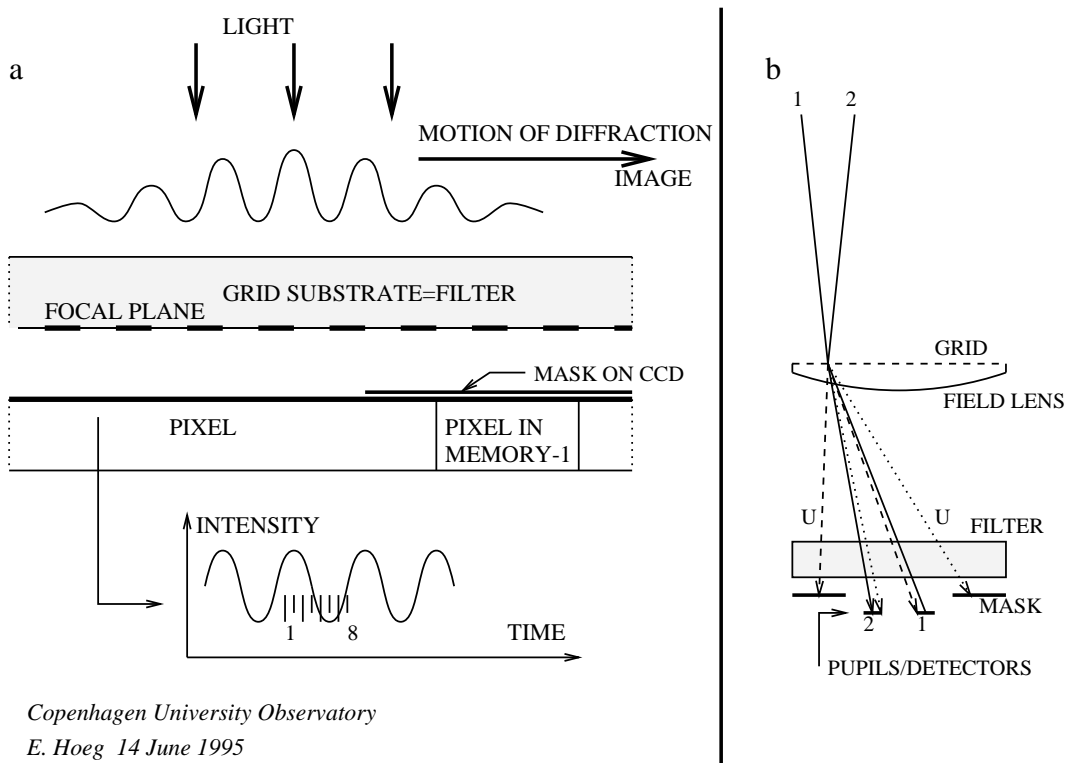


Figure 1: Principle of light modulation by an amplitude grid. (a) the proposed layout of a grid close to the CCD. It will produce a sinusoidal intensity modulation to be sampled at 8 points. (b) the layout by LP where a field lens forms images on the detectors of the telescope pupils that contain the modulated light. The unmodulated light, however, of one of the 1st order spectra of each pupil ($U-U'$) is stopped by the mask.

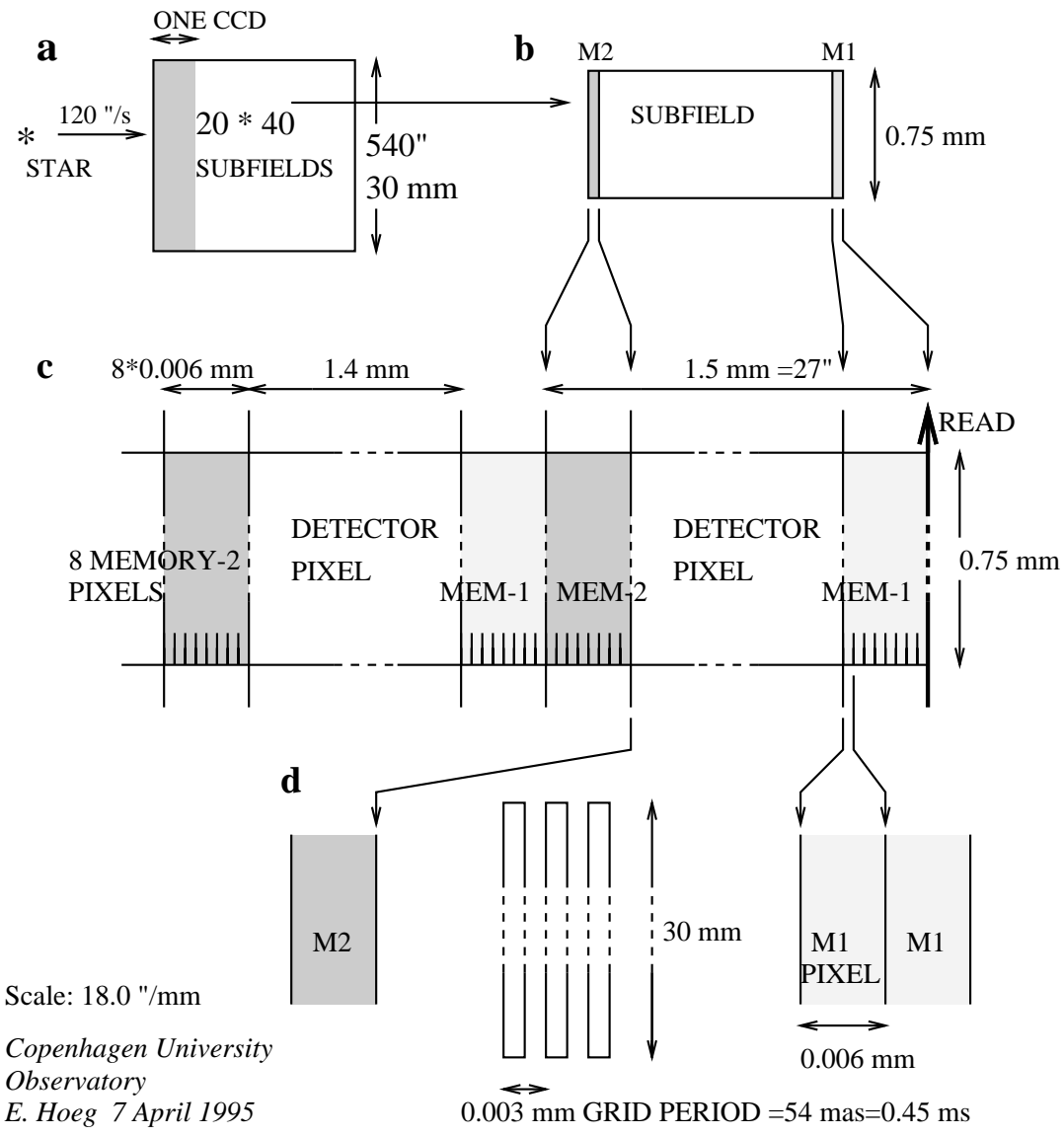


Figure 2: Detector for an amplitude grid. (a) layout of the grid for one of the 32 fields in the focal plane of GAIA; one of the CCDs is indicated. (b) one of the 800 subfields covered by CCD pixels. (c) pixels enlarged. (d) the shaded area of all memory pixels are covered with a mask, an opaque layer, so that only the detector pixels remain sensitive to light.

Since the modulation period depends on the slightly variable rotation speed of the satellite great care must be taken that the integration of the modulation curves are in phase. This synchronization requires that the rotation speed be known in real time with an accuracy of $\simeq 10^{-4}$ if 1000 periods are superposed. Each time 8 points of the modulation curve have been accumulated all useful charges will be located in the $M1$ pixels, Fig. 2. A waiting period of any desired length is permitted at such times and will be used for synchronization. The length of all waiting periods must be recorded with the resulting samples. The charges located in $M2$ and in the detector pixels at the waiting times are not useful and they are quickly skipped during the later readout process.

The required attitude control for the similar ROEMER mission proposed for the ESA M3 mission by Lindgren et al. (1993) was discussed by F. van Leeuwen in Annex B of that report.

2.1. The Integration Strategy

All operations of a CCD may be described in detail by a few elementary processes. The passive process of doing nothing is called 'waiting' if the useful charges are placed in $M1$, and is otherwise called 'integration', thus named after the purpose. The duration, T , may be specified by writing `wait(T)` or `integrate(T)` and it shall include the time for any subsequent shifting of charges.

The active process 'left' shifts all charges towards left in Figs. 2 and 3, with the additional result that the pixels adjacent to the read register are zeroed. Repeating this process n times is written `left*n`, with reverse Polish notation. The process 'right' shifts all charges to the right and zeroes all pixels with the highest number at the very left. Finally, 'read' pushes all charges in the read register, i.e., the rightmost column in Fig. 2c, by one unit towards an output amplifier where the first charge is converted to a digital number. All processes have a duration time called the process interval, e.g., the 'left interval' and the 'right interval' which are about 0.001 ms.

Compound processes are defined in these terms for the specific observation strategy required. Thus for the detector being described here:

$$1 \text{ octo process} = [\text{wait}(T1) + \text{left} * 8] + [\text{integrate}(T2) + \text{right}] * 8 \quad (1)$$

as illustrated in Fig. 3. Octo processes are repeated $N4$ times, as specified below, in a compound process:

$$1 \text{ detection process} = \text{octo} * N4 \quad (2)$$

Reading is performed by

$$1 \text{ readout process} = (\text{right} + \text{read} * 40) * 8 + \text{right} * 9 \quad (3)$$

giving $40*8=320$ samples because there are 40 horizontal rows of subfields. The samples consist of the content of the rightmost memory-1 at the beginning of a readout. The content of the detector pixel and of memory-2 at that time is not useful information and is skipped by the

process 'right*9'. It appears that memory-2 is needed during readout, but not especially during the integration. These processes are finally combined into:

$$1 \text{ frame process} = \text{wait}(T0) + \text{detection} + \text{readout} \quad (4)$$

After a readout process all charges have been shifted 17 pixels towards right. This means that a new detection process will accumulate charges onto charges from previous detections.

The light from any given star will contribute to two modulation curves, i.e., to 2×8 samples. We may speak of a 'drift scan modulation detector', similar to the simple drift scan used in the incoherent imaging outer part of the field of view.

The observation or charge integration strategy is somewhat similar to the star observing strategy of Hipparcos (Perryman & Hassan 1989, p. 18), but is much simpler because the parameters are not star-dependent and can be controlled by the on-board computer. The strategy for each CCD, illustrated in Fig. 3, is built around a time hierarchy corresponding to the above defined processes and the following definitions:

(1) the waiting interval, $T1 \simeq 0.009$ ms, includes the time required for synchronization ($\simeq 0.001$ ms), and the time for 8 shifts left;

(2) the integration interval, $T2 = 0.055$ ms, is the constant time during which charges are accumulated in a detector pixel, adding to previously accumulated charges, before being shifted into memory, cf. Fig. 2c;

(3) the octo interval, $T3 = T1 + T2 * 8 \simeq 0.45$ ms, is closely equal to the modulation period and therefore slightly variable in order to match the actual variations of the rotation speed of the satellite;

(4) the detection interval, $T4$, is the total time allocated to accumulation of charges before readout of the CCD. It corresponds to a star image motion of 27 arcsec, i.e., the width of a subfield. We have $T4 = T3 * N4 \simeq 216$ ms if $N4 = 480$;

(5) the readout interval, $T5 = 320 \times t_R = 6.4$ ms, if $t_R = 0.02$ ms, cf. Sect. 2.3;

(6) the frame interval, $T6 = T0 + T4 + T5 = 225$ ms, is the time allocated for waiting, detection and readout. It should be exactly the time it takes the star to cross a subfield so that the new accumulation is in phase with previous ones. This synchronization is obtained by proper choice of $T0$.

2.2. Grid and CCD

The grid and the CCD for a field are mounted nearly in contact, separated by perhaps 0.10 mm. The grid has a period about 0.003 mm, equal to the fringe spacing at the wavelength defined by the colour filter. The grid thus contains 10000 vertical slits each with the area 0.0015×30 mm².

The field is covered by a chip with several CCDs, Fig. 2a, each corresponding to N_c columns of 40 subfields. If we assume $N_c = 4$ each field could contain 4 CCDs, allowing

the width of one subfield as spacing between the CCDs on the chip. The samples thus correspond to N_c detection processes.

The star light has to pass through the grid substrate, which may also act as the colour filter required to limit the bandwidth to about 200 nm as proposed by LP. This arrangement requires a good optical quality of the substrate which should not be difficult to achieve. In the LP proposal, shown in Fig. 1b, this is not required because the filter is placed close to the exit pupils. Similarly, the uniformity of the CCD must be higher in the present proposal. But an averaging of non-uniformities is achieved because the stars move along the pixels and because they cross many different pixels along different lines. If the separation of grid and CCD is eg. 0.10 mm the (monochromatic) light of a star in the 0th and 1st orders would be spread over 4 equidistant circles of 0.005 mm diameter since the aperture ratio of the beams is 1:20. The circles, or short spectra of the pupils, are spaced by an angle of $2.5/11.5 = 0.22$ radian since the baseline of the interferometer is 2.5 m and the focal length is 11.5 m. This corresponds to 0.022 mm on the CCD.

The disadvantages of the present proposal are perhaps outweighed by the greater simplicity. No field lenses are required that could be difficult to manufacture and to adjust in the right position relative to the mask in Fig. 1b. The efficiency of the present proposal is not as high as that of the amplitude grid shown in LP-Fig. 6A because the unmodulated light in the 1st order spectra at U-U is included. In the proposal by LP the unmodulated light is always stopped by the masks. It should be noted that the images at U are in principle modulated, namely by the 2nd order image from the other entrance pupil. For an amplitude grid, however, the second order image has zero intensity. This is not true for the phase grid where the U-images are therefore modulated.

The required masking of the memory pixels has been successfully tried on frontside CCDs, but not on backside illuminated ones where the alignment would be more difficult. Evaporation of an interference filter on a backside illuminated CCD is probably possible.

2.2.1. Some Detector Problems

A problem of the CCD as described was pointed out by Fred Harris (1995, priv. comm. at USNO, Flagstaff Station). Each detector pixel has an area about $1 \times 1 \text{ mm}^2$, much larger than usual pixels which may be up to $50 \times 50 \mu\text{m}^2$. A certain voltage gradient is required to shift the charges from pixel to pixel and this gradient would be excessively large for the proposed size of detector pixel. Three conceptually different solutions to this problem were suggested.

One solution is to divide the CCD detector pixels into a number of more narrow pixels in the direction of motion. After an integration interval, $T_2 = 0.055$ ms, the charges are concentrated by shifting into one memory pixel. From there they are multiplexed and summed at proper phase into one of eight memory pixels.

Another solution is to use a hybrid technique of photodiodes and CCDs. Each photodiode at the place of a detector pixel is connected to a CCD read register. The phase-correct accumulation is then done either in a digital computer or in 8 CCD memory pixels.

A third solution is also a hybrid with photodiodes. The Charge Modulation Device (CMD) is described by Nakamura & Matsumoto (1991) and manufactured by Olympus Optical Co., Tokyo. The CMD would seem interesting for space astrometry for its potentially high operating speed, small pixel size ($5 \mu\text{m}$), and low power consumption, but it can only be used in stare mode; not for drift scan.

Thus, all these solutions work without the proposed left shifting of charges; all accumulation of charges is done in memory, not in the detector pixel. Space on the chip for required memory is readily available in the detector design #2, cf. Fig. 4.

2.2.2. Cosmic Ray Damage

Another problem especially of large CCD pixels is that they would be liable to gradual damage by cosmic rays during the lifetime. David Lumb (1995, priv. comm.) notes: "The method of repeated forward and backward clocking has serious consequences for the performance, especially in the regime of radiation damaged CCDs. Charge traps will be building up during the lifetime. Depending on the charge packet size and the clock timings there will be a complicated relation for the trapping probabilities. However the repeated back and forward clocking is typically used as a method of diagnosing CCD damage because it very efficiently highlights where traps occur, by repeated filling of the trap, and subsequent release to following charge packets. Very obvious charge streaks appear in normal CCD flat fields so operated. For the GAIA case the depth of modulation and possibly even the phase information would be distorted. This would need very careful assessment." – This problem may perhaps be solved by one of the hybrid techniques mentioned in Sect. 2.2.1, none of which use repeated clocking in the CCD.

2.3. Readout Noise and Input Catalogue

The question of readout noise shall be discussed because of its importance for the optimal choice of the width of the CCDs, i.e., for N_c , and also for the question whether a large input catalogue is required for the mission. A small input catalogue of about a million stars is required for determination of the real-time satellite attitude, but we want to see whether a large input catalogue containing all say 50 million program stars is also required in order to observe faint stars of about $V = 15$ mag without an excessive noise introduced by the readout.

The readout of a sample is accomplished in a time t_R and it will introduce a noise σ_R in the sample which is larger for small values of t_R . If a sample contains N_e e^- from the star and background the total statistical error σ_S of the sample is given by

$$\sigma_S^2 = N_e + \sigma_R^2 \quad (5)$$

Typical pairs of values in units of [0.001 ms, 1 e^-] are $(t_R, \sigma_R) = (1, 10; 5, 7; 20, 4; 100, 2; 200, 1.5; 450, 1)$, according to R.F. Nielsen (1993, priv. comm.).

For a star of $V = 15$ we can expect a count rate in GAIA of about 1160 electrons/s behind an amplitude grid and

a colour filter. The light from a star will be distributed on 16 samples because a given star may accumulate light onto two detector pixels during a single detection process. This means on average $N_s = 1160 \cdot T4/16 \cdot N_c$ electrons per sample. A choice of $N_c = 4$ and $t_R = 0.02$ ms is reasonable since it gives a readout noise of $\sigma_R^2 = 16 \ll N_s = 58$. Thus the readout of all samples permits a sufficiently small readout noise.

The corresponding readout interval of 6.4 ms is very small compared to the 225 ms frame interval.

It is noted that an input catalogue of 50 million stars gives an average of 0.034 star/subfield. Since each star affects two subfields during a frame interval about 7 percent of these are affected. If an input catalogue were used during readout only 7 percent of the samples would have to be read as ‘slowly’ as mentioned. The rest could be quickly skipped thus saving time for a larger t_R for the useful samples. But this saving is not necessary.

It seems therefore that with respect to readnoise a large input catalogue would not be mandatory for the interferometric part of the mission. But it has been said in discussions of this paper that the above assumptions on readnoise are optimistic in a space environment.

3. DETECTOR DESIGN #2 – FOR A PHASE GRID

The above detector design #1 without field lenses is not suited for a phase grid since the modulation in the two pupils are shifted in phase by π . The combined light is therefore unmodulated.

Field lenses are required to image the two pupils on different detectors. This is achieved by the optical system in Fig. 4. Cylinder lenses perpendicular to the motion of the stars shown in 4a and 4b, image the pupils on separate detector pixels. This is shown at lower right for the two stars A and B. The pupils are normally elongated as shown for A because the image is only sharp perpendicular to the cylinder lens. One of the pupils for B is divided into two narrower images because the figure shows the moment when a beam passes from one lens to the next. In practice the junction between lenses is probably not very sharp because of manufacturing imperfections. But this is not critical provided the junction is sufficiently uniform along the lenses.

The detector pixels can here be only 0.25 mm wide as shown in Fig. 4b, thus easing the problem discussed in Sect. 2.2.1 and allowing more space for the memory pixels.

The observation is carried out by a detection process during an interval $T4$ as defined in Eq. (2). The reading shall produce two modulation curves corresponding to the two pupils. The frame process Eq. (4) is thus changed into

$$1 \text{ frame process} = \text{wait}(T0) + \text{detection} + \text{readout} * 2 \quad (6)$$

The light from a star is therefore normally distributed on $4*8$ samples per CCD. In some cases the light is divided among pixels in two horizontal rows, e.g., if the star A would run 0.2 mm higher on the CCD. This happens in about 20 percent of all observations for which $8*8$ samples per CCD are then required. Therefore, about 10 percent of all samples contain useful information on the 50 million program stars.

3.1. Data Rates

The data rates for the phase grid in design #2 are 640 samples per frame per CCD. (This is twice the rates for the amplitude grid in design #1.) A frame interval is $T6 = 225$ ms; there are 4 CCDs per field, according to Sect. 2.2, and 32 fields in each of the 3 telescopes proposed for GAIA, in total $3 * 32 * 4 = 384$ CCDs. The total rate is accordingly

$$R = 384 \cdot 640/0.225 \simeq 1.1 \cdot 10^6 \text{ samples/s} \quad (7)$$

for the interferometric part of GAIA, independent of the number of program stars. We have not counted the records of all the waiting intervals $T1$ which must be taken into account in calculating the phases, but since they are common for one or several CCDs they can probably be neglected in an account of the amount of data. We assume that 12 bits per sample gives sufficient accuracy when a semi-logarithmic code is used in the transmission to the ground. The transmission of all samples would thus require 13 Mbits/s.

Since this is too much to transmit a reduction by on-board processing is required. An input catalogue of the 50 million stars could be used to extract the relevant samples and to process them which would reduce the data rate.

We shall define a *transit* as the result from one subfield consisting of $2 \cdot 8$ samples, or the resulting phase, amplitude and background, resulting from a processing. Let us organize the transmission in telemetry formats of $T_f = 10$ s duration, as for Hipparcos¹. A format would on average contain coherent observations of $n = 4050$ stars from a total of 3.3 square degrees from the three telescopes. During a format a star will cross a maximum number of $T_f/T6/N_c = 11$ CCDs, or on average 8 CCDs, each integrating $4 \cdot T6 = 0.9$ s, cf. Sect. 2.2 and Fig. 2a. On each of the CCDs two subfields will be affected, giving $8 \cdot 2$ transits. But sometimes two rows of pixels are affected, giving about 20 transits per star per format, or 880 bits per star, including the header. This results in a data rate of $n \cdot 20/T_f$ processed transits per second or **360 kbits/s**, if all relevant information from each CCD is transmitted.

About 500 kbits/s is a high, but probably acceptable data rate from a geostationary orbit, according to W. Flury, ESOC. And since also data from the incoherent imaging has to be transmitted, further reduction seems required.

¹The format header contains basic information for the subsequent star records: time, attitude, attitude rates, waiting times $T1$, etc. The star records also contain such information, but given relative to the header information and therefore requiring a smaller number of bits. The star header contains in about 160 bits: the star identification number, 28 bits; the predicted values for the first transit of: scan velocities in w, z , i.e., along scan and perpendicular, 16+16 bits; position angle of CCD, 16 bits; time of transit after the format time, up to 10 s with resolution 0.1 μ s, 28 bits; number of the CCD, 10 bits; number of row of pixels on CCD, 8 bits; various flags, 6 bits.

The transit records for the coherent observations follow in sequence of time and each contain in about 36 bits: the actual number of the row of pixels, relative to the number in the header, 3 bits; observed phase, 12 bits $\simeq 14 \mu$ as resolution; observed amplitude, 12 bits; observed background, 9 bits.

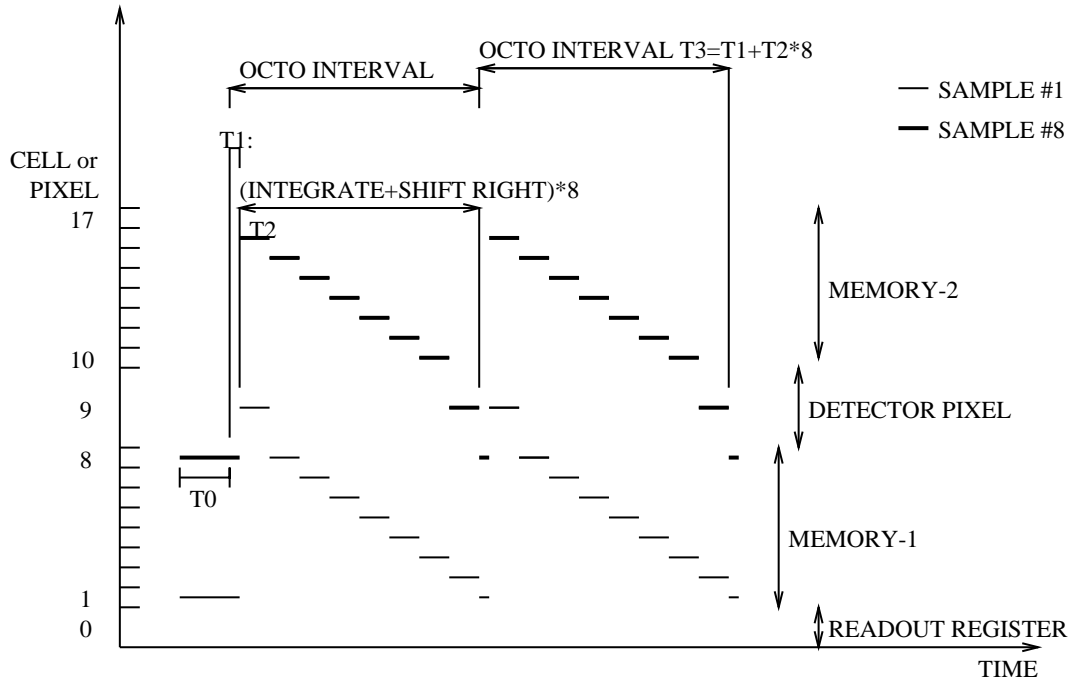


Figure 3: Integration strategy for GAIA detector. The samples #1-8, cf. the modulation curve in Fig. 1a, result from integration in short intervals of length $T_2=0.055$ ms. See Sect. 2.1 for further explanation.

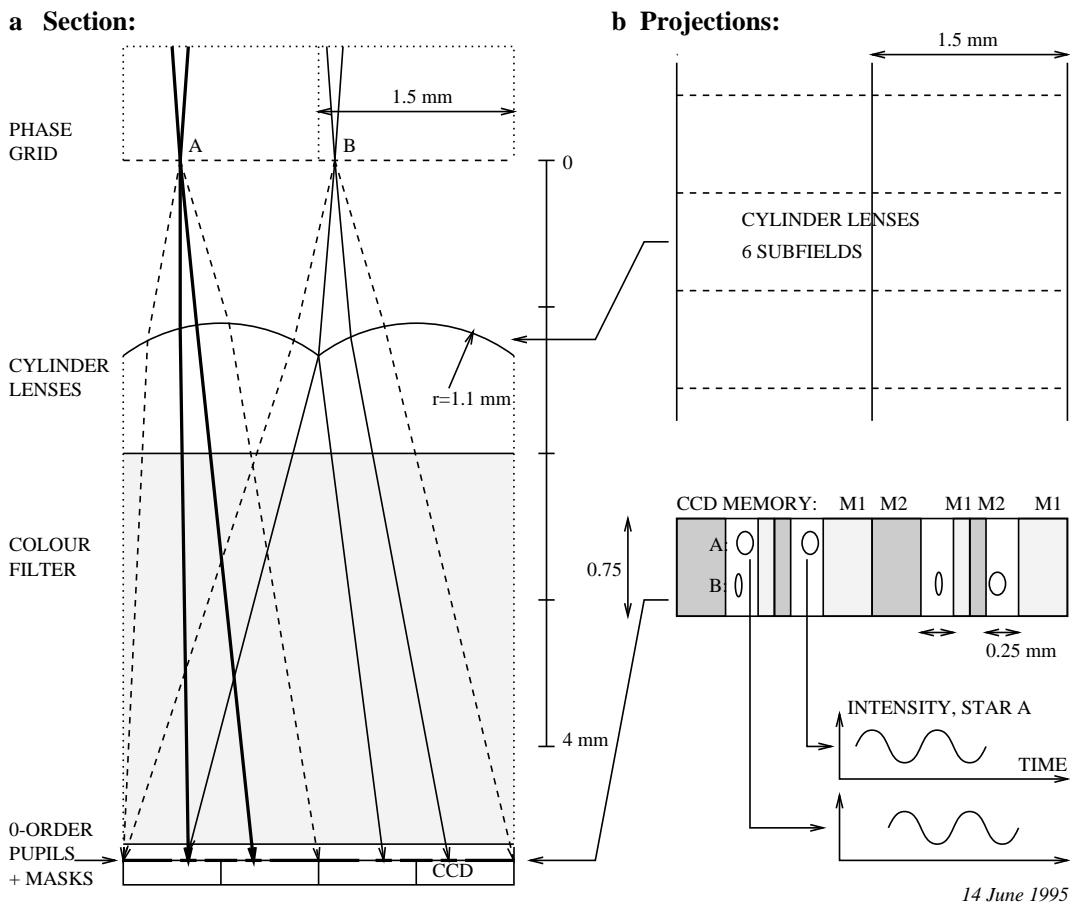


Figure 4: Detector for a phase grid as 'drift-scan modulation detector'. (a) a section of the grid with two stars A and B; (b) projections of the cylinder lenses, and four detector pixels with masks. Charges are shifted horizontally. At lower right the intensity of the two pupils of star A is shown with the phase shift of π , characteristic for a phase grid.

14 June 1995

It might be possible to take data for a star from subsequent subfields together, and also data for a star from the four CCDs on each chip. A further reduction of transmission by a factor 0.25 might be possible. It is therefore reasonable to allocate **250 kbits/s** of telemetry to the coherent mode of observation.

The on-board processing might take the signal-to-noise ratio into account. If a significant modulation is detected, larger than a given limit of signal-to-noise ratio, the data might be transmitted, even if it does not belong to any star of the input catalogue. A provisional star number must be given for such cases.

3.2. Optimization for the Phase Grid

We have adopted the size of the subfield from LP and believe that it is fairly optimal. A final optimization would require consideration of the width and height of the subfields, of N_c , and of the size of the field. The spacing between grid and field lenses is also a free parameter, but the focal length of the field lens follows herefrom when we require that the 1st order U-images are separated by the width of the field lenses, as in Fig. 4a. There are no other parameters to optimize for a given telescope and interferometer design.

3.3. Charge Transfer

The charges of a sample has been subject to a large number of shifts before readout, namely

$$N_{\text{shift}} = 16 \cdot N4 \cdot N_c = 30720 \text{ shifts/sample} \quad (8)$$

A shift does not transfer the charges completely, a small fraction remains in neighbouring pixels. This phenomenon is described by the charge transfer efficiency, CTE . We shall assume today's current value of $CTE = 0.999994$ although improvement to 0.999998 is expected by the CCD techniques of the next few years. The total efficiency in our case is $E = CTE^{N_{\text{shift}}/2} = 0.91$ taking into account by division with 2 that the whole charge is accumulated during these shifts. The resulting effect is a slight reduction of the modulation amplitude but no effect on the phase is expected. The value of 0.91 means that no significant loss is expected from this source.

But David Lumb (1995, priv. comm.) notes: "The design makes excessive demands on CCD CTE . This factor will be dominated by in-orbit damaged generated traps, and not by intrinsic performance." - This problem and tentative solutions are discussed in Sects. 2.2.1. and 2.2.1.

4. CONCLUDING REMARKS

The problems of larger pixels, cf. Sect. 2.2.1, and of radiation damage must be solved.

The proposed detector systems are simpler than that proposed by LP; which does not say that the proposed detector is really simple. The efficiency of design #2 for the phase grid seems to be nearly as assumed by LP in calculating their Table 3 of performances. But we should allow for a loss of 20 percent light between the 4 CCDs on a chip and a further 10 percent loss at the junctions of

fields lenses and during shifting of charges. Therefore the errors given for the baseline option in LP-Table 3 should be multiplied by 1.15 to obtain the errors expected for design #2.

The design #1 for an amplitude grid is the simpler one since no field lenses are required. The standard errors of LP-Table 3 only take photon statistics into account. They should therefore be multiplied by about $1.15 \cdot 1.3\sqrt{2} = 2.1$ where the factor $\sqrt{2}$ accounts for the loss of 50 percent of the light in an amplitude grid and the factor 1.3 tentatively accounts for the inclusion of the unmodulated 1st order images in the integrated light.

We shall define a single observation as an observation from one CCD and give expressions to obtain the standard errors of such a single observation. The 384 CCDs (see Sect. 3.1) proposed above for GAIA will obtain about 17 interferometric observations per CCD for a given star in a 5 year mission, or a total of $N_{\text{5int}} = 6528$ observations. It can be shown that the errors of parallax given in LP-Table 3, col. 2, should be multiplied by $\sqrt{N_{\text{5int}} * 0.5} / 1.19 = 48$ to obtain the average error of a single one-dimensional astrometric observation.

The corresponding numbers related to the incoherent observations in LP-Table 4 are 21.6 observations per CCD chip, and the 3 telescopes contain a total of 36 W-band CCDs for astrometry and 3 CCDs per band for photometry. The factor to be applied with LP-Table 4 is therefore approximately 16.6 for astrometry. There will be about 64 observations per photometric intermediate band so that a factor $\sqrt{64}$ should be applied to the errors in LP-Table 4 for w, u, \dots, I to obtain the standard errors of single observations.

ACKNOWLEDGEMENTS

This work was supported by the Danish Space Board. The author is grateful for useful discussions and for comments to previous versions of this paper by Drs C. Fabricius, F. Harris, L. Lindegren, D. Lumb, V.V. Makarov and M.A.C. Perryman.

REFERENCES

- Høg E., Lindegren L. 1993, A CCD modulation detector for a second Hipparcos mission, in: *I.I. Mueller and B. Kolaczek (eds.) Developments in Astrometry and Their Impact on Astrophysics and Geodynamics, IAU Symp. No. 156*, 31.
- Lindegren L. (ed.) 1993, *ROEMER - Proposal for the Third Medium Size ESA Mission (M3)*, Lund.
- Lindegren L., Perryman M.A.C. 1994, GAIA - Global Astrometric Interferometer for Astrophysics, in *Supplementary Information Submitted to the Horizon 2000+ Survey Committee*, 52pp.
- Nakamura T., Matsumoto K. 1994, Present status and future prospects of CMD image sensors, in: *OPTOELECTRONICS - Devices and Technologies* Vol. 6, No. 2, 261-277
- Perryman M.A.C., Hassan H. 1989, *The Hipparcos mission*, Vol. 1, *The Hipparcos Satellite*. ESA Publications Division, ESA SP-1111.